Design of the CHARIS integral field spectrograph for exoplanet imaging

Groff, Tyler, Peters, Mary Anne, Kasdin, N. Jeremy, Knapp, Gillian, Galvin, Michael, et al.

Tyler D. Groff, Mary Anne Peters, N. Jeremy Kasdin, Gillian Knapp, Michael Galvin, Michael Carr, Michael W. McElwain, Timothy Brandt, Markus Janson, James E. Gunn, Robert Lupton, Olivier Guyon, Frantz Martinache, Nemanja Jovanovic, Masahiko Hayashi, Naruhisa Takato, "Design of the CHARIS integral field spectrograph for exoplanet imaging," Proc. SPIE 8864, Techniques and Instrumentation for Detection of Exoplanets VI, 88640H (26 September 2013); doi: 10.1117/12.2025081

Event: SPIE Optical Engineering + Applications, 2013, San Diego, California, United States

Design of the CHARIS Integral Field Spectrograph for Exoplanet Imaging

Tyler D. Groff[a], Mary Anne Peters[a], N. Jeremy Kasdin[a], Gillian Knapp[a], Michael Galvin[a], Michael A. Carr[a], Michael W. McElwain[b], Timothy Brandt[a], Markus Janson[a], James E. Gunn[a], Robert Lupton[a], Olivier Guyon[c], Frantz Martinache[c], Nemanja Jovanovic[c], Masahiko Hayashi[d], Naruhisa Takato[c]

[a]Princeton University, Princeton, NJ USA [b]Goddard Space Flight Center, Greenbelt, MD USA [c]Subaru Telescope, Hilo, HI USA [d]National Astronomical Observatory of Japan, Mitaka, Tokyo Japan

ABSTRACT

Princeton University is building an integral field spectrograph (IFS), the Coronagraphic High Angular Resolution Imaging Spectrograph (CHARIS), for integration with the Subaru Coronagraphic Extreme Adaptive Optics (SCExAO) system and the AO188 adaptive optics system on the Subaru telescope. CHARIS and SCExAO will measure spectra of hot, young Jovian planets in a coronagraphic image across J, H, and K bands down to an 80 milliarcsecond inner working angle. SCExAO's coronagraphs and wavefront control system will make it possible to detect companions five orders of magnitude dimmer than their parent star. However, quasi-static speckles in the image contaminate the signal from the planet. In an IFS this also causes uncertainty in the spectra due to diffractive cross-contamination, commonly referred to as crosstalk. Post-processing techniques can subtract these speckles, but they can potentially skew spectral measurements, become less effective at small angular separation, and at best can only reduce the crosstalk down to the photon noise limit of the contaminating signal. CHARIS will address crosstalk effects of a high contrast image through hardware design, which drives the optical and mechanical design of the assembly. The work presented here sheds light on the optical and mechanical considerations taken in designing the IFS to provide high signal-to-noise spectra in a coronagraphic image from and extreme adaptive optics image. The design considerations and lessons learned are directly applicable to future exoplanet instrumentation for extremely large telescopes and space observatories capable of detecting rocky planets in the habitable zone.

Keywords: Extreme Adaptive Optics, Coronagraphy, Exoplanets, Broadband, Integral Field Spectrograph

1. INTRODUCTION

CHARIS is a lenslet based imaging spectrograph designed specifically for detecting and characterizing exoplanets, brown dwarfs, and debris disks. It has a low dispersion mode that provides a spectral resolution of $\lambda/\Delta\lambda \sim$R15 from 1.15 to 2.4 microns, and a high dispersion mode that is designed for a resolution greater than R60 in J, H, and K bands. CHARIS will be located behind the SCExAO instrument and the AO188 adaptive optics system on the Nasmyth platform of the Subaru telescope, as shown in Fig. 1(a).

The CHARIS assembly, shown in Fig. 1(b), is an all reflective design that produces high quality images over the entire 1.15-2.4 micron bandpass and mitigates spectral cross-contamination, or crosstalk, to less than 1% over any spectral bandpass. There are two dispersion modes using one 3-element prism for the high resolution mode, and a second 3-element prism for the low resolution mode. The critical design review is scheduled for October 2013. Delivery to the telescope and commissioning will begin in the winter of 2015 and 2016. We present an overview of the science case, optical design, and mechanical design of the instrument.

Send correspondence to Tyler Groff tgroff@princeton.edu

Techniques and Instrumentation for Detection of Exoplanets VI, edited by Stuart Shaklan, Proc. of SPIE Vol. 8864, 88640H · © 2013 SPIE · CCC code: 0277-786X/13/$18 · doi: 10.1117/12.2025081

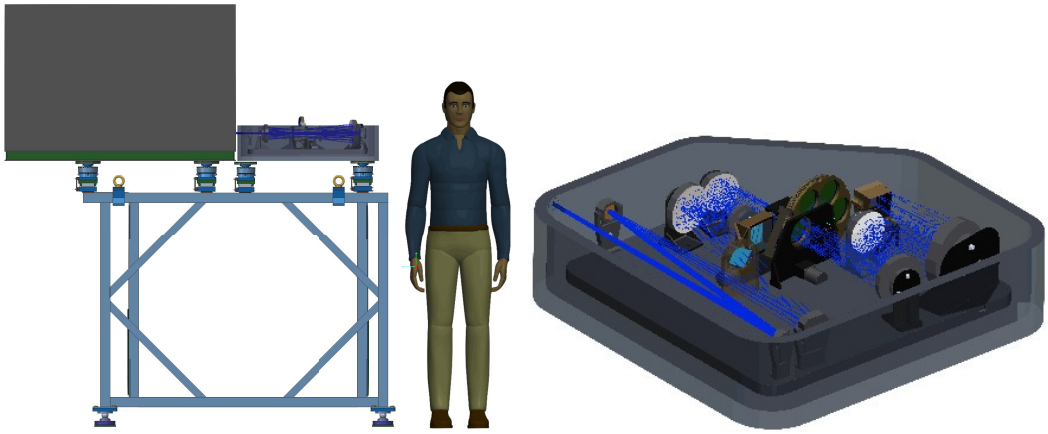

(a) CHARIS+SCExAO on Observation Frame (b) CHARIS Assembly with the dewar lid off

Figure 1. CHARIS on the observation frame behind SCExAO, and an iso-view of the instrument inside of its dewar with the lid off.

2. SCIENCE CASE AND REQUIREMENTS

CHARIS will observe in the northern sky, but the closest moving groups to Earth with relatively young systems (∼1-10Myears) where we expect planet formation are predominantly accessible in the southern sky. For this reason, many major exoplanet imaging instruments, such as SPHERE and GPI, will be located at the Chilean observatories. However, some of these moving groups, such as Orion and Upper Scorpius, are also accessible in the northern hemisphere[1] and some are only accessible in the northern hemisphere, such as Castor, Ursa Majoris, and Hercules Lyra. Indeed, HR8799 is most easily observed in the northern sky and the only imaging spectrograph designed specifically for exoplanets that is currently on sky, P1640, is in the northern hemisphere.[2] With a combination of high (∼R80) and low resolution (∼R15) observations, CHARIS will constrain exoplanet masses and atmospheric conditions. The spectral information will help eliminate false positives, improving the scheduling of revisits and increasing the number of targets we can visit. Increasing the number of observable targets in the northern sky and expanding the coverage of 8-meter class ExAO systems to the entire sky will help to uncover the frequency of exoplanet systems and establish the dependence of exoplanet formation on the host star's age and metalicity.[3] The combination of relatively old (∼100 Myear) and young (∼1 Myear) systems accessible to the northern hemisphere provides a rich sample set that is as yet inaccessible. More of these targets will be accessible thanks to the anticipated <80 milliarcsecond inner working angle and high throughput given by the SCExAO Phase Induced Amplitude Apodization (PIAA) coronagraph,[4] combined with the high sensitivity of Subaru's AO188[5,6] adaptive optics system (which can provide good Strehl ratios down to a magnitude R=16.5 star) and the high throughput design (>70%) of CHARIS. Currently SCExAO+CHARIS is the only planned instrument in the northern hemisphere implementing multiple coronagraphs, broadband wavefront control, and an imaging spectrograph onto an 8-meter class telescope. In high resolution mode, CHARIS can spectrally characterize a target in J, H, and K bands. In low resolution mode, CHARIS will provide spectral measurements from 1.15 to 2.4 microns. Since many moving groups in the northern hemisphere are so far away, such measurements are important to eliminate revisits separated by many years to check for common proper motion.

One interesting science trade was whether or not to include Y-band in the CHARIS design. In the end we chose not to include Y-band within CHARIS, which was driven in part by feedback from the resulting instrument performance. The principal function of Y-band was disk science and the study of clouds in young giant exoplanet atmospheres. The distinction between clear and cloudy atmospheres increases with decreasing wavelength, and is thus larger in the Y-band than in J, H, or K. However, this is a smooth function of wavelength, and is already substantial in J-band. Indeed, much of the recent science on clouds in brown dwarf atmospheres has been achieved in the J-band rather than in Y-band[7,8] due to the better instrument performance in the J band. The scientific impact of Y-band is limited compared to J, H, and K bands, and the optical performance will be modest even with SCExAO+CHARIS in Y-band due to the rapid drop in achievable Strehl ratio as a function of wavelength. Most importantly, the inclusion of Y-band resulted in an expected degradation of spectral cross-

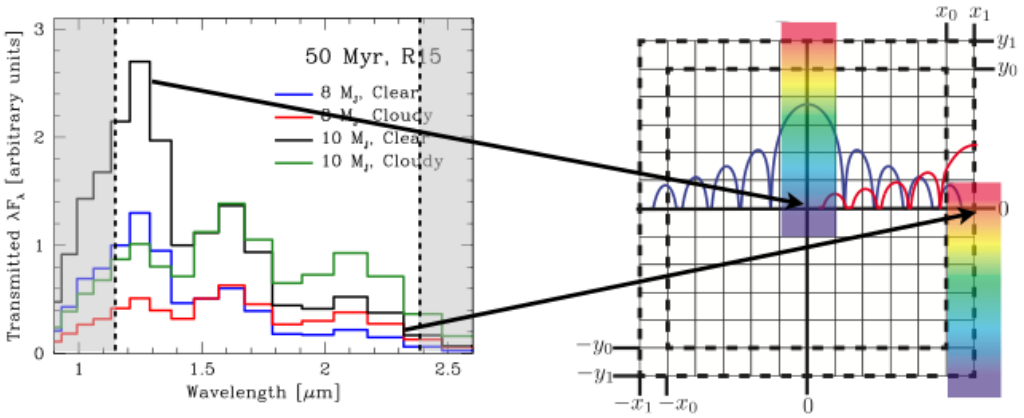

Figure 2. Example showing the issue of adjacency between the long and short wavelengths in the low-resolution mode, which exhibit approximately a factor of ten variance in brightness.

contamination, and the field of view suffered from having to Nyquist sample a shorter wavelength. Since Y-band measurements need not be taken within a cryogenic instrument SCExAO will provide a high Strehl-ratio beam to a suite of dedicated short wavelength instruments. Other instruments being included in SCExAO,[9] such as FIRST[10] and VAMPIRES,[11] are designed specifically for disk science and the formation of planets within them. Overall, eliminating Y-band from CHARIS increased the field of view from 1.75 to 2.07 arcseconds, relaxed the optical requirements (and hence improved its expected performance over the new band), and resulted in a highly complementary suite of instruments that are all optimized for the science in their respective bandpasses.

Spectral contamination, or crosstalk, between adjacent lenslets is a fundamental limitation in the spectral certainty provided by an integral field spectrograph. Every planet will be Nyquist sampled by the lenslet array, which means that the light from that planet will be sampled by four adjacent lenslets. As a result, the planet can contaminate its own spectrum since the short wavelengths are closely packed to the long wavelengths, as indicated in Fig. 2. To keep spectral self-contamination below 1%, we must show robustness to the expected spectral variance of a distribution of planets in each bandpass. From the warm start planet models given by

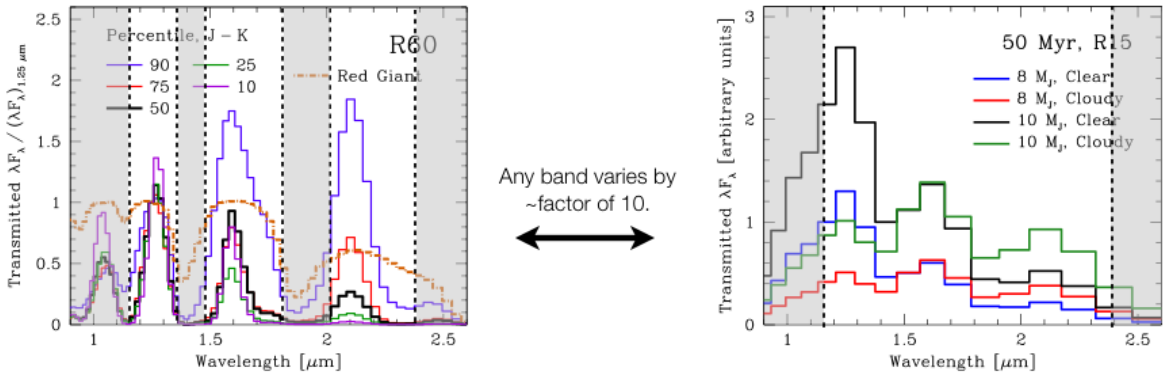

Figure 3. Example spectra of an exoplanet as predicted by the Spiegel and Burrows warm start model.[12](a) distribution of color profiles as predicted by the warm start model measured at a spectral sampling of R60 at each of the J, H, and K bandpasses. (b) Example spectra sampled at R15, sampled over the 1.15-2.4 micron low-resolution mode. In any bandpass or planet model, there is as much as an order of magnitude difference in the signal from the planet.

Spiegel and Burrows,[12] shown in Fig. 3, we expect there to be approximately one order of magnitude variation between the shortest and longest wavelength in any bandpass that a planet is observed. This makes the crosstalk constraint stricter, and from Fig. 2 we see that this derives from the adjacency of the short and long wavelengths in adjacent spectra. Thus, to guarantee $< 1\%$ spectral contamination between the blue and red ends of the spectrum, the intensity of light from any wavelength must must be $< 1 \times 10^{-3}$ of its peak power at the onset of the next spectrum (which is ~ 90 microns in the CHARIS design).

3. OPTICAL OVERVIEW

The purpose of an integral field spectrograph is to measure the spectrum over the entire field of view in a single image. To do so we rely on a lenslet array to create sparsity in the broadband coronagraphic image so that there is adequate space between each spatial sample for dispersing their spectra without overlap. The sparse image is collimated and a 3-element prism disperses the field prior to being re-imaged onto an H2RG detector. The spectral range, wavefront requirements, ghost suppression over such a large bandpass, and most importantly the diffractive crosstalk requirement drives the imaging and relay optics to an all reflective design (apart from the prism and lenslet array), shown in Fig. 4. The design temperature range is $\approx 70-100$ Kelvin, at $\leq 10^{-6}$ Torr. The optics upstream of the lenslet array are Zerodur spherical optics with passively athermalized mounts to maintain surface figure and minimize scatter incident on the lenslet array. The collimator and camera optics are heritage passively athermalized diamond turned aluminum made by L-3 SSG and have slightly more complicated conic sections to minimize design residuals so that the crosstalk effects will remain as diffraction limited as possible. All reflective surfaces are coated with protected gold to maximize the throughput over the entire 1.15-2.4 micron bandpass. The lenslet array Nyquist samples the F/420 primary image formed by the two spherical telescope

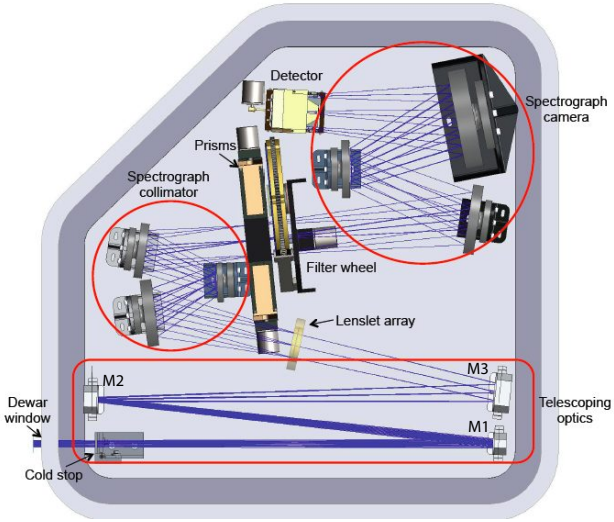

Figure 4. Top view of the entire CHARIS layout. The telescope optics, M1 and M2, are immediately after the cold stop. M3 is a flat fold mirror that redirects the F/420 primary image onto the lenslet array. The three-mirror collimation assembly feeds the light into the prism, which disperses the field prior to going into the three-mirror camera optics. The dispersed image, whose bandpass is defined by the filter choice is imaged by a Teledyne H2RG detector.

optics, shown prior to the M3 fold mirror in Fig. 4. The lenslets are F/8 with a 250 micron pitch, which produces a sparsely sampled version of the incident F/420 image. Once this image is collimated, dispersed, and re-imaged, there are approximately 90 microns between adjacent spectra on the detector. Details of the optical design that went into the choice of the spectral length, and the optical design tradeoffs that lead us to such a fast lenslet with a large pitch are provided in Peters-Limbach et al.[13] Indeed many interesting changes in the design choices outlined here and in Peters-Limbach et al.,[13] such as the implications of the bandpass on the physical parameters of the lenslet and relay optics, have been made since Peters et al.[14] One of the more significant choices was to not include a Y-band imager within CHARIS, as discussed in §2, but we have also been able to increase the speed of the relay optics so that the wavefront requirements could be relaxed. Excluding Y-band from CHARIS has dramatically improved the quality of the field going into the relay optics, has simplified anti-reflection coatings and filter sets, and has increased the field of view to a 2.07x2.07 arcsecond field of view. The CHARIS prisms, shown in Fig. 5, are designed to provide high and low resolution spectra across the J,H, and K bands. The low resolution is designed to disperse from 1.15-2.4 microns, and will allow us to take spectra at the approximate resolution and bandwidth shown in the R15 plot in Fig. 3. The high resolution prism is designed for a higher

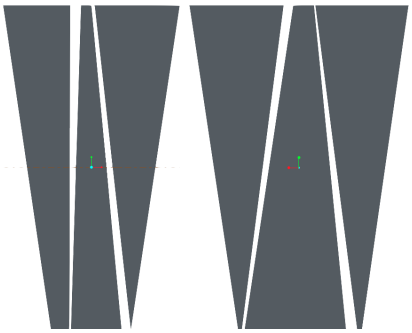

(a) Low Resolution Prism (b) High Resolution Prism

Figure 5. CHARIS (a) low and (b) high resolution prisms. The middle element of both prisms is made from LBBH-1, with BaF2 for the first and third elements (CaF2 is also an option).

degree of dispersion, so that it may be used for J,H, and K bands. The minimum spectral resolution required of the high resolution prism for each bandpass (defined by the gray areas) is shown in the R60 plot of Fig. 3. Detailed spectral resolution curves for the prisms are given in Peters-Limbach et al.[13] Note that the prisms have been designed to closely match in angular deviation, which we have chosen to be zero so that we may attempt to flat field the detector and image in an undispersed mode (for calibration). This allows for us to include a set of periscope optics to relay the beam around the lenslet array. This will allow for on-sky flat-fielding of the detector, an option that does not exist with current IFS designs.

To maintain the crosstalk requirements set forth in §2, spectral contamination must be controlled on several fronts. The first is diffractive contamination from the discrete sampling provided by the lenslet array, for which we are using an array of field stops to block this diffractive contamination.[15,16] Mechanically we must maintain the relative position of these field stops to micron level precision across the entire lenslet array from 293 to ∼77 Kelvin. Thus, the field stops are printed directly on the back of the lenslet array in black chrome. Peters-Limbach et al.[13] shows that the diffractive effects of the pinhole not being located at the exact image plane for each wavelength has no appreciable affect on the crosstalk requirement. After the lenslet array the design residuals, expected optical surface figure, and expected alignment error of the collimator and camera must be controlled to keep the spot size incident on the detector as close to the diffraction limit as possible. This is done by levying requirements on the ensquared energy and power spectral density of the optical system. Drawing

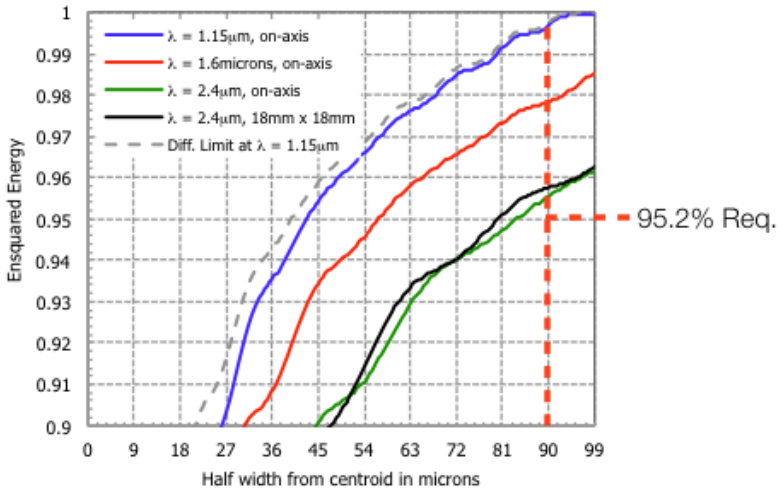

Figure 6. Expected Ensquared energy of the collimator and camera sub-assemblies at different field points and wavelengths, including design residuals and an approximation for the expected residual wavefront error at the pupil plane.

from the warm start models shown in Fig. 3, an ensquared energy of $> 95.2\%$ will guarantee that the brightest point in the planets spectrum will not contaminate the dimmest point by more than 1%. This requirement derives from defining the ensquared energy as a function of the contrast, and assuming that all of the remaining energy is contained within the next spectra (a conservative assumption). In the end, the optical performance for the collimator and camera optics and the pinholes on the back side of the lenslet array satisfy this minimum requirement with a small amount of margin.

4. OPTOMECHANICS

Since CHARIS images out to 2.4 microns, the instrument is held at cryogenic temperatures. The detector must be held at 77 Kelvin or below, and the relay optics have a gradient constraint that keeps the entire instrument at these temperatures. This is also for the safety of the detector, so that it is not the coldest point in the dewar and there is a large thermal mass to damp warming and cooling transients. This also damps out the temperature fluctuations on the detector, which has a significant effect on the time-varying component of the read noise on the detector. The optomechanical design of the instrument is tailored to balance the required alignment precision against mechanical stability and thermal grounding so that it will hold alignment from room temperature down to 77 Kelvin. The two Zerodur spherical optics that form the primary image on the lenslet

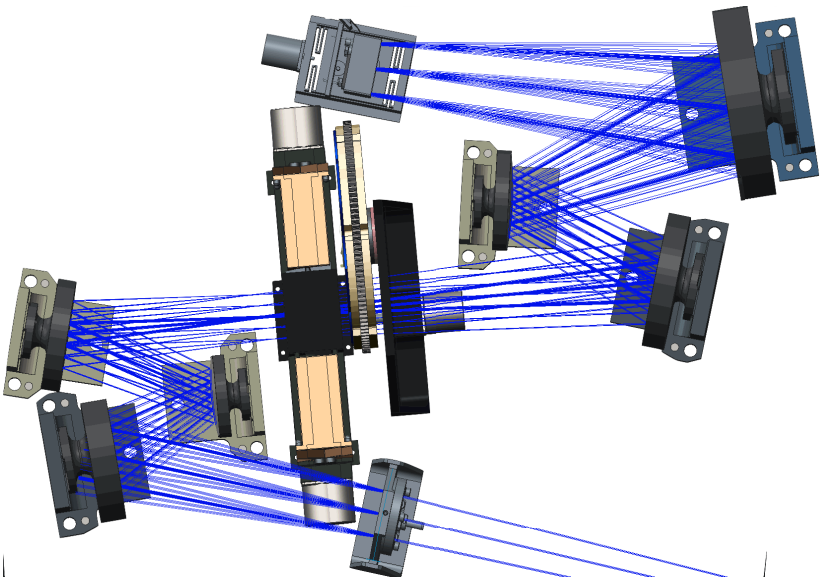

Figure 7. Optomechanical layout of the collimator, prism, filter, camera, and detector assemblies

array are held in flexure mounts to minimize any mechanical stressing of the optical surface as the aluminum housing thermally contracts. These mounts, shown in Fig. 8(a), are constructed with vertical positioning only. The mechanism is a polished aluminum friction slider that is preloaded with Belleville washers. A high pitch screw is used to precisely adjust the height of the optic. The Belleville washers were chosen so that they may be fully compressed, maximizing the preload within the mount after alignment. The vertical slider is intentionally very long to maximize both precision and thermal contact. Overall this simplification of the mechanism reduces cold mass, increases stability, and improves the inherent rigidity of the system during operation. Since the optic is spherical, the vertical positioning also allows us to finely control tip-tilt. It has been determined that lapping the bottom of these mounts during warm tests will be sufficient to get the optic well within the maximum stroke of the vertical stage.

The lenslet array mount, shown in Fig. 8(b), has the opposite mechanism type relative to the spherical optic mounts. In this case the lateral tolerance of the lenslet array is quite loose since it is slightly oversized relative to the field of view defined by the detector. Since the lenslet array is only sampling the primary image formed by the two spherical optics, there is no central axis of the optic that must be aligned with the chief ray. Thus, we

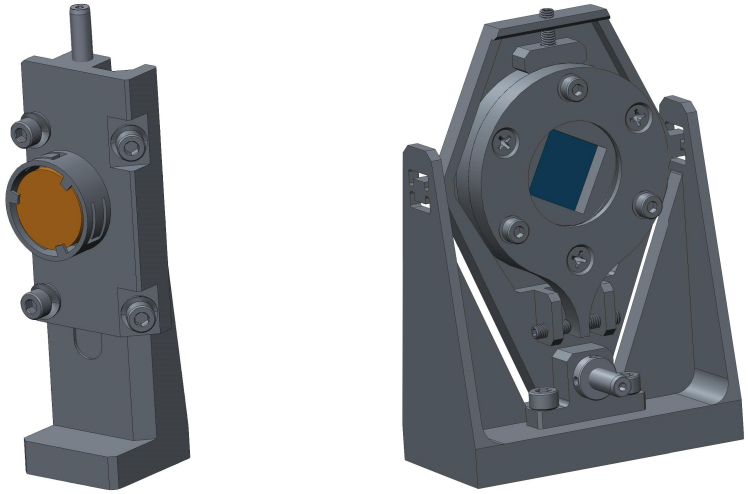

(a) M1 Mount (b) Lenslet Array Mount

Figure 8. Optical Mounts for the telescope optics, which have translation control, and the lenslet array, which has tip-tilt control.

may rely on machining precision for the vertical placement of the lenslet array. However, the performance of the collimator and camera optics is highly dependent on how well the incident field is coupled into the collimator. The entire lenslet array must be within 10 microns of the incident plane, which exceeds the lapping capability. Thus, a precision tip-tilt mount was included in the lenslet array mount.

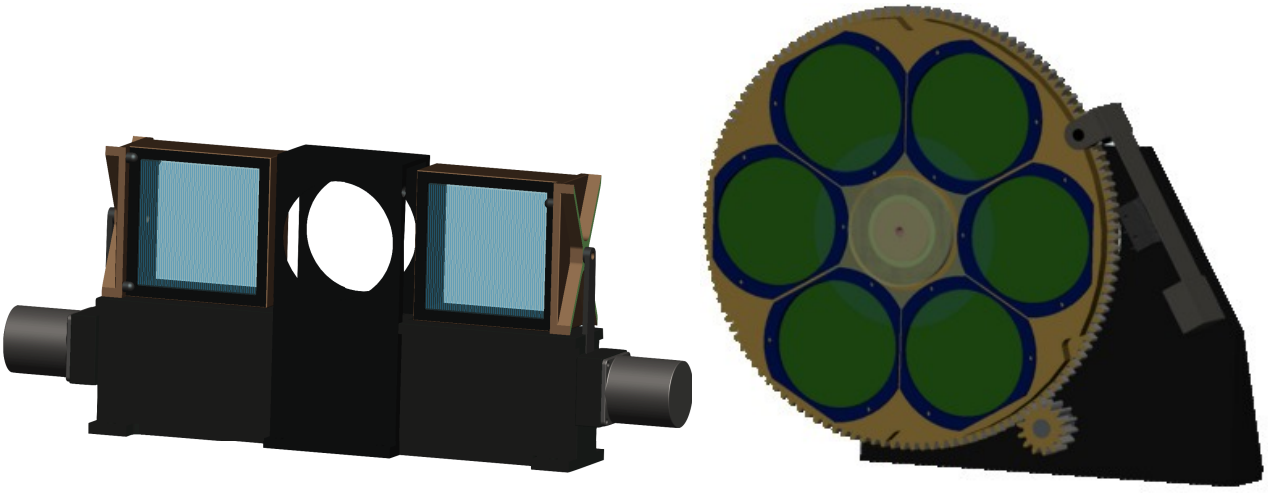

(a) Prism Slider (b) Filter Wheel

Figure 9. Prism and Filter Mechanisms

The relative clocking of the prism, lenslet, and detector is also quite important, particularly the clocking between the lenslet array and the prism slider. There are two prisms, however, and each moves into position via a linear slider mechanism, shown in Fig. 9(a). Each prism has a 3-point kinematic mount that locates it in position and angle relative to the beam. This provides a high degree of precision and repeatability for the prism position in the beam, while allowing the linear slider to be relatively loose so that it does not bind as the mechanism is taken down to temperature. The prisms are located once, and we rely on machine precision to orient their position relative to the collimation and camera optics. With this fixed, the lenslet array may be manually clocked to the correct orientation relative to the prism with a high precision friction rotation ring. Once in position the rotation stage, which is very similar in design to the sliders on M1 and M2, can be locked

down to maintain a high degree of stability. The procedure and isolation of rotation mechanisms is critical to meeting the crosstalk requirements highlighted in §2 and §3, and also discussed in Peters-Limbach et al.[13]

5. SUMMARY

CHARIS is a high contrast imaging integral field spectrograph designed to provide spectra from 1.15 to 2.4 microns. It will be located behind the SCExAO instrument and AO188 adaptive optics system on the Nasmyth platform of the Subaru Telescope. One of the primary design considerations in CHARIS is to mitigate spectral crosstalk between adjacent spectra. Such a constraint does sacrifice field of view, but is not a limiting constraint for a coronagraphic instrument. The instrument is designed to constrain spectral contamination from a source that is one order of magnitude brighter than the object of interest to less than 1%. This is achieved by depositing an array of field stops on the back side of the lenslet array, and controlling the wavefront residuals of the collimation and camera optics. The strict alignment and stability levels associated with these requirements drives decisions on the optomechanics and alignment procedures. Wherever possible, we choose greater stability using rigid mounts over mechanisms. We also require high degree of repeatability from our mechanisms, particularly the prism slider's angle and position tolerances in the closed position. Such requirements maintain the spectral crosstalk levels below their acceptable limit, and also minimize post-processing errors that would arise from what appear to be complex registration errors at the detector plane. The strict requirement on crosstalk suppression in the CHARIS hardware, without relying on post-processing, is one of the defining characteristics of this instrument. It is a unique problem for high contrast imaging in particular, where we are attempting to detect inherently faint spectral signals from the planet in the presence of a bright speckle field from the star the planet is orbiting.

Acknowledgements

The CHARIS spectrograph is funded by the National Astronomical Observatory of Japan.

REFERENCES

1. L. Malo, R. Doyon, D. Lafrenière, É. Artigau, J. Gagné, F. Baron, and A. Riedel, "Bayesian analysis to identify new star candidates in nearby young stellar kinematic groups," *The Astrophysical Journal* **762**(2), p. 88, 2013.
2. B. Oppenheimer, C. Baranec, C. Beichman, D. Brenner, R. Burruss, E. Cady, J. Crepp, R. Dekany, R. Fergus, D. Hale, *et al.*, "Reconnaissance of the hr 8799 exosolar system. i. near-infrared spectroscopy," *The Astrophysical Journal* **768**(1), p. 24, 2013.
3. M. McElwain, T. Brandt, M. Janson, G. Knapp, M. Peters, A. Burrows, A. Carlotti, M. Carr, T. Groff, J. Gunn, O. Guyon, M. Hayashi, N. Kasdin, M. Kuzuhara, R. Lupton, F. Martinache, D. Spiegel, N. Takato, M. Tamura, E. Turner, and R. Vanderbei, "Scientific design of a high contrast integral field spectrograph for the subaru telescope," in *Proceedings of SPIE*, **8446**, p. 84469C, 2012.
4. O. Guyon, F. Martinache, R. Belikov, and R. Soummer, "High performance piaa coronagraphy with complex amplitude focal plane masks," *The Astrophysical Journal Supplement Series* **190**, p. 220, 2010.
5. Y. Minowa, Y. Hayano, S. Oya, M. Watanabe, M. Hattori, O. Guyon, S. Egner, Y. Saito, M. Ito, H. Takami, *et al.*, "Performance of subaru adaptive optics system ao188," in *Society of Photo-Optical Instrumentation Engineers (SPIE) Conference Series*, **7736**, p. 122, 2010.
6. S. Egnera, Y. Ikedab, M. Watanabec, Y. Hayanoa, T. Golotaa, M. Hattoria, M. Itoa, Y. Minowaa, S. Oyaa, Y. Saitoa, *et al.*, "Atmospheric dispersion correction for the subaru ao system," in *SPIE Astronomical Telescopes and Instrumentation: Observational Frontiers of Astronomy for the New Decade*, pp. 77364V–77364V, International Society for Optics and Photonics, 2010.
7. É. Artigau, S. Bouchard, R. Doyon, and D. Lafrenière, "Photometric variability of the t2. 5 brown dwarf simp j013656. 5+ 093347: Evidence for evolving weather patterns," *The Astrophysical Journal* **701**(2), p. 1534, 2009.

8. J. Radigan, R. Jayawardhana, D. Lafrenière, É. Artigau, M. Marley, and D. Saumon, "Large-amplitude variations of an l/t transition brown dwarf: multi-wavelength observations of patchy, high-contrast cloud features," *The Astrophysical Journal* **750**(2), p. 105, 2012.
9. O. Guyon, F. Martinache, C. Clergeon, R. Russell, T. Groff, and V. Garrel, "Wavefront control with subaru coronagraphic extreme adaptive optics (scexao) system," in *Proceedings of SPIE*, **8149**, p. 814908, 2011.
10. E. Huby, G. Perrin, F. Marchis, S. Lacour, T. Kotani, G. Duchêne, E. Choquet, E. Gates, J. Woillez, and O. Lai, "First, a fibered aperture masking instrument: on-sky results," in *SPIE Astronomical Telescopes+ Instrumentation*, pp. 84461Z–84461Z, International Society for Optics and Photonics, 2012.
11. B. R. Norris, P. G. Tuthill, M. J. Ireland, S. Lacour, A. A. Zijlstra, F. Lykou, T. M. Evans, P. Stewart, T. R. Bedding, O. Guyon, *et al.*, "Probing dusty circumstellar environments with polarimetric aperture-masking interferometry," in *SPIE Astronomical Telescopes+ Instrumentation*, pp. 844503–844503, International Society for Optics and Photonics, 2012.
12. D. Spiegel and A. Burrows, "Spectral and photometric diagnostics of giant planet formation scenarios," *The Astrophysical Journal* **745**(2), p. 174, 2012.
13. M. Peters-Limbach, T. D. Groff, N. J. Kasdin, D. Driscoll, M. Galvin, A. Foster, M. Carr, D. LeClerc, R. Fagan, M. McElwain, G. Knapp, T. Brandt, M. Janson, O. Guyon, N. Jovanovic, F. Martinache, M. Hayashi, and N. Takato, "The optical design of charis: An exoplanet ifs for the subaru telescope," in *Proceedings of SPIE*, **8864**, 2013.
14. M. Peters, T. Groff, N. Kasdin, M. McElwain, M. Galvin, M. Carr, R. Lupton, J. Gunn, G. Knapp, Q. Gong, A. Carlotti, T. Brandt, M. Janson, O. Guyon, F. Martinache, M. Hayashi, and N. Takato, "Conceptual design of the coronagraphic high angular resolution imaging spectrograph (charis) for the subaru telescope," in *Proceedings of SPIE*, **8446**, p. 84467U, 2012.
15. B. Woodgate, E. Mentzell, G. Hilton, and D. Lindler, "An integral field spectrograph design concept for the terrestrial planet finder coronagraph," *New Astronomy Reviews* **50**(4), pp. 297–300, 2006.
16. D. Bonfield, B. Woodgate, C. Grady, G. Hilton, L. White, and J. McCleary, "Gfp-ifs: a coronagraphic integral field spectrograph for the apo 3.5-meter telescope," in *SPIE Astronomical Telescopes+ Instrumentation*, p. 70146W, 2008.